

Computer-Aided Detection of Polyps in CT Colonography Using Regional Textural Features

Önder Demir

Abstract— Colorectal cancer is a serious health problem in the developed countries and is one of the leading causes of mortality due to cancer. Early detection is important to reduce for preventing death. However, early diagnosis of polyps in computerized tomography colonography (CTC) images is a difficult process because of the difficulties of distinguishing them from non-lesion structures. In this study, a computer aided detection (CAD) system for detection of polyps in CTC images is presented to help radiologists. The developed system consists three phases; preprocessing phase, feature extraction phase and classification phase. In preprocessing phase, CTC images are enhanced, then region of interests (ROI) and volume of interests (VOI) are identified. In feature extraction phase, morphological, statistical and textural features extracted from ROIs and VOIs. Textural features are divided into two categories: extracted from inside of the polyp and extracted from outer surface of the polyp. Three different classifier are used in the last phase for decision. The developed system reaches 96.7% sensitivity rate. Experimental results indicates that the developed scheme is useful to detect polyps and decrease number of false positive in CTC images.

Keywords— Computer-aided detection, computed tomographic colonography, polyp detection, textural features, image processing.

I. INTRODUCTION

Colorectal cancer is the third most common cancer and comes the second in cases of cancer resulting in death [1], [2]. The structures which grow abnormally on the inner surface of the intestinal wall tissue are called as "polyps". Originally non-cancerous polyps can become cancerous lesions over time. Detection and removal of polyps before they turn into a malignant structure greatly reduces the risk of developing colorectal cancer [2], [3]. Patient satisfaction is low due to the implementation way of optic colonoscopy, which is one of the current methods for imaging polyps [4]. Besides, polyps are difficult to detect through colonography videos due to the fact that they have different forms, textures, sizes and locations. Computed tomography colonoscopy (CTC) is highly successful in computer-assisted detection of polyps. CTC also provides higher patient satisfaction at cheaper cost. Computer-aided design (CAD) systems shorten the time it takes radiologists to review CT images and increase the rate of correct detection [4], [5].

Various CAD systems were developed for the detection of polyps in CTC images. The general structure of these CAD

systems consists of colon segmentation, feature extraction, and classification steps, which determine whether the polyp is a lesion or not [4]. The success of the colon segmentation process is significant for the success of the system. Incorrect segmentation can delay the process, leading to unnecessary inspection of structures that cannot be polyps. It may also hinder the detection of real polyps. Li et al. performed colon segmentation, using a two-dimensional region growing algorithm on each CT slice image [6]. In literature, other studies are available for two-dimensional segmentation. Chowdury and Whelan developed a method for colon segmentation, using geometric features. The method they developed reached a sensitivity rate of 98.04% [7]. 3-D segmentation based on conjunct evaluation of consecutive slices can provide better results. There are two important steps in three-dimensional segmentation. The first step is the determination of the starting point of the process on the target region and expansion of the region to be segmented into the desired size. At this point, two methods come to the forefront in general: the border-based method and the region-based method. In their study, Wyatt et al. performed colon segmentation using 3-D region growing technique, starting from the points they detected on binary images. In literature, there are also studies where colon segmentation was performed using different methods [8].

Manjunath et al. performed colon segmentation on CT images using a knowledge-based method [5]. Manjunath and Siddalingaswamy used a post-processing method to perform contrast enhancement without losing textural details [9].

For feature extraction, Hu et al. used Haralick's texture identification features for 3-D space. They applied the Karhunen-Loeve (KL) transformation on these features to obtain new features and classified those by random forest algorithm [10]. Ren et al. aimed to reduce the number of false positives by using new morphological features in their study [11]. Xu and Suzuki tried to form the cluster of features with the best results. They did it by classifying the 75 2-D and 3-D features into their subsets using SVM and linear discriminant analysis methods [12]. By using the random forest algorithm, Bae and Yoon identified the most selective ones among the 33 different types of features [13]. In this study, the morphological features, statistical and textural features of polyps in CT images are extracted and classified by different classification algorithms.

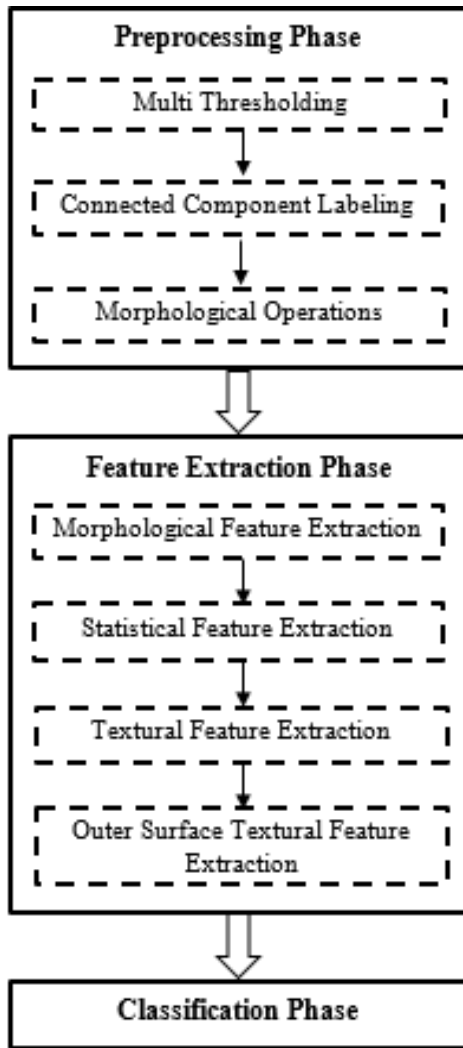


Fig. 1. Block diagram of the developed system.

In the second part of the paper, the pre-processing, feature extraction and classification stages of the developed system are described. The experimental results are presented in the third part. In the last part, the results obtained are discussed and information about future studies is given.

II. THE DEVELOPED SYSTEM

The developed system consists of three stages as; pre-processing, feature extraction and classification. In the first stage, which is the pre-processing stage, multiple gray level density thresholding, neighborhood labeling and morphological operations are performed. In the feature extraction stage, statistical, morphological and textural features of the regions of interests, which are determined by labeling, are extracted. In the last stage, classification is performed using these features. A block diagram of the system developed is shown in Fig. 1.

A. Pre-processing Stage

Gray level intensity thresholding is a technique used in many image processing applications. In thresholding process, pixel values forming the image matrix, which are lower or higher than a certain value, are equalized to another value.

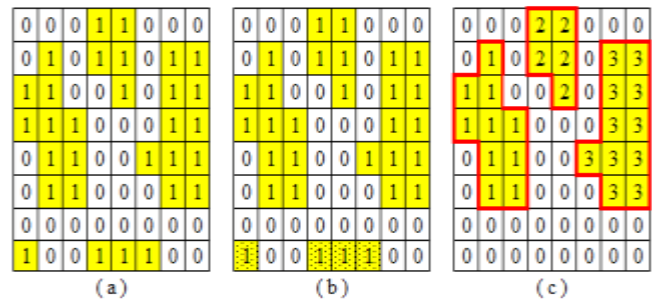


Fig. 2. Steps of connected component labeling

Thus; regions with undesired density values are removed from the image. Multiple thresholding can be used if the pixels forming the target region are within a certain value range.

Pixels which are lower than the minimum density threshold (indicating the lower limit) and which are higher than the maximum density threshold (indicating the upper limit), are assigned "0" value so that these regions can be removed from the image [14]. After this process, the image is converted into a binary image, making it suitable for morphological operations and morphological feature extraction.

Connected component labeling on binary images is performed by marking the neighbor pixels of value "1" with the same label number as the adjacent neighbor pixels of value "1". This procedure is performed for all elements of value "1", from the (0, 0) element of a binary image matrix of $m \times n$ size to the $(m-1, n-1)$ element. The process for a label continues until there is no new neighbor pixel of value "1". All objects on the binary image are numbered and marked in this way [15], [16]. An example of connected component labeling is shown in Fig. 2. In Fig.2 (a), a binary image matrix is shown. More than five connected "1" valued pixels are marked on Fig.3 (b). The label matrix for appropriate connected neighborhoods is shown in Fig.2 (c).

The pixel values in the same coordinates as these label values are accessed through the actual image. The actual pixel values are used to calculate statistical features.

After labeling process, morphological operations are performed on the binary image. The aim of morphological operations is to facilitate the identification of structures that may be region of interest for feature extraction. Erosion and closing operations are applied sequentially using appropriate structure elements. First, morphological erosion is performed to separate the polyp candidates from the intestinal wall. Then, the morphological closing process is applied to fill the gaps formed after the erosion. In Fig.3 (a), an original CTC image is shown. Binary image after thresholding process is shown in Fig.3 (b). Detected region of interests are marked on binary image and original image after morphological operations in Fig.3 (c) and (d) respectively.

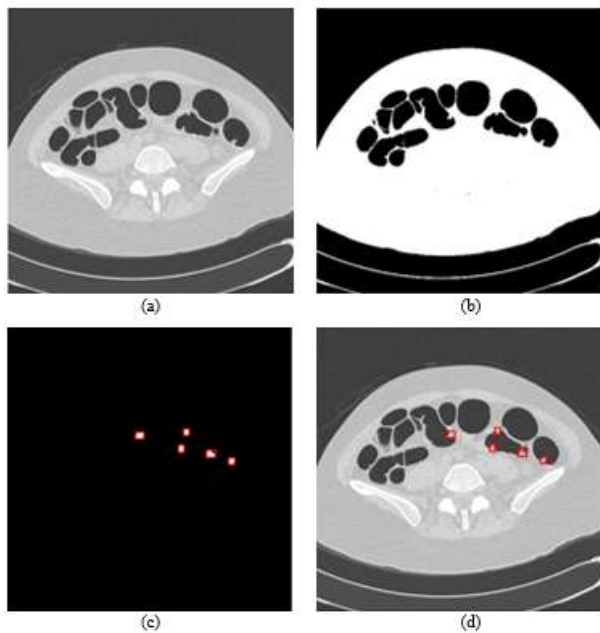


Fig. 3. (a) Original CTC image (b) Binary image after thresholding (c) Region of interests on after morphological operations (d) Marked region of interests on original CTC image

B. Feature Extraction Stage

The system extracts three different kinds of features, which are extracted from a region of interest. These are statistical, morphological and textural features. Textural features are extracted from 2 different regions of the polyp; which are the inside of polyps and outer surface.

Four different kinds of morphological features are extracted by the system. These features are listed in Table I.

TABLE I: LIST OF MORPHOLOGICAL FEATURES

No	Morphological Features
1	Area
2	Minimum Axis Length (MinAL)
3	Maximum Axis Length (MaxAL)
4	MinAL / MaxAL

Area(A): Area is the number of pixels that make up a volume of interest. The number of elements with the same label as the region of interest in the label matrix gives this value.

Minimum Axis Length (MinAL): The minimum distance between the two pixels, which form the boundary of the region of interest.

Maximum Axis Length (MaxAL): The maximum distance between the two pixels, which forms the boundary of the region of interest.

MinAL / MaxAL: This is the ratio of the minimum axis length to the maximum axis length.

The eight statistical features shown in Table II are extracted by the system. These features are extracted from the original image using the coordinates in the label matrix of the regions of interest [17], [18].

TABLE II: LIST OF STATISTICAL FEATURES

No	Statistical Features
1	Mean Value
2	Maximum Pixel Value
3	Minimum Pixel Value
4	The Most Frequent Pixel Value
5	Variance (σ^2)
6	Standard Deviation (σ)
7	Skewness (γ)
8	Kurtosis (K)

Mean Value: This is the arithmetic mean of all pixels that make up the region of interest.

Maximum Pixel Value: This is the highest value among the pixel values that make up the region of interest.

Minimum Pixel Value: This is the lowest value among the pixel values that make up the region of interest.

The Most Frequent Pixel Value: This is the most frequent value among the voxel values that make up the volume of interest.

Variance: This is a measure that intends to determine the scale or propagation of the values in the cluster of pixel values. For all the values inside the cluster of variance samples, the averages of the squares of distances from a specific value or the mean value, are calculated.

Standard Deviation: This is a measure that is used to summarize the propagation of the values in a cluster of pixel values.

Skewness: Skewness is the measure of the symmetry of the distribution of values in a cluster of pixel values. If the skewness is less than zero, the histogram of the values is skewed to the left. If it is equal to zero, the histogram is symmetrical and if bigger than zero, then the histogram is skewed to the right.

Kurtosis: Kurtosis is a measure indicating the sharpness or kurtosis of the histogram showing the distribution of the values in a cluster of pixel values.

Two different methods are used to extract the textural features. One is Haralick's Gray Level Co-occurrence Matrix (GLCM) and the other is Gabor's filters. With these methods, features are extracted separately from the inner surface and outer surface of the polyp candidate [19], [20].

The GLCM is created by examining the positions and values of two pixels comparatively. In this examination, the basis pixel is called the reference pixel, and the second pixel available in the defined distance and direction, is called the target pixel. The direction and distance used in this examination is important for creating the GLCM. GLCM can be created according to the neighbors of the reference pixel, which are located at different distances in eight directions. This direction and distance are determined by examining the textural pattern in the image. All the GLCM should be created by examining the same direction and distance. The examination can be done with one of the adjacent neighbors, or with a neighbor pixel located at a distance specified by a distance vector marked by symbol 'd'

[20]. Table III shows reference pixel, distance vector and target pixel samples.

TABLE III: REFERENCE AND TARGET PIXEL EXAMPLES

Reference Pixel	Distance Vector	Target Pixel
(4, 4)	(0, 2)	(4, 6)
(3, 5)	(2, 2)	(5, 7)
(10, 14)	(1, 0)	(11, 14)
(20, 10)	(3, -3)	(23, 7)

For example, if the adjacent pixel on the right of the reference pixel is to be examined, the distance vector is specified as (0, 1), i.e., the east. The target pixel is reached by incrementing the row number by 0 and the column number by 1 according to the coordinate of the reference pixel. In the image matrix, all pixels from the upper left corner to the lower right corner are sequentially examined as reference pixels. At the end of this examination, the GLCM elements specify the number of pixels possessing their row and column number values. The element on the first row and first column of the GLCM shows the number of neighborhoods where both the reference pixel and the target pixel are of value "1" in the examined texture image. Fig. 4 shows the calculation of the GLCM from a texture image matrix [14]. In order to reduce the element values of GLCM, which is a statistical probability matrix, from 0 to 1, normalization is performed by dividing each element by the sum of matrix values. Calculation is made with the normalization equation (1) where the "Co_{i,j}" indicates the GLCM element on row i. and column j.

$$P_{i,j} = \frac{Co_{i,j}}{\sum_{i,j=1}^n Co_{i,j}} \tag{1}$$

Numerous features defining the characteristics of textural patterns can be extracted from the GLCM matrices. Five of these features were selected in order to define the textural patterns on polyps. Table IV shows the features calculated using the GLCM formed by the neighborhood analysis of this matrix.

TABLE IV: LIST OF GLCM FEATURES

No	Textural Features
1	Contrast (Con)
2	Energy (Ene)
3	Entropy (Ent)
4	Homogeneity (Hom)
5	Moment (Mom)

Contrast: The GLCM contrast value, which is different from a normal digital image contrast value, indicates the difference between the target pixel and the reference pixel in the textural pattern examined. The GLCM contrast value is calculated by (2). For a GLCM of size G*G, i and j indicate the GLCM row and column number, and Co(i, j) indicates the value of the GLCM element in those coordinates.

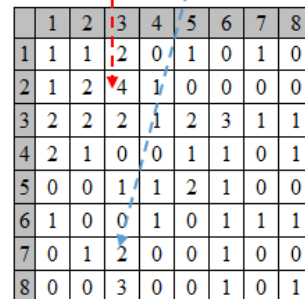
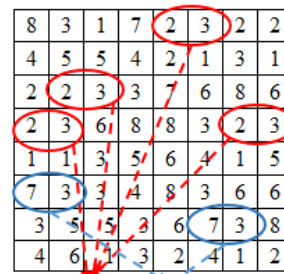


Fig. 4. Calculation of the GLCM Matrix

$$Con = \sum_{i=0}^{G-1} \sum_{j=0}^{G-1} Co(i, j) - (i - j)^2 \tag{2}$$

Energy: The energy is the measure indicating the uniformity of a texture. A high energy value can be obtained in uniformly sequenced matrices where the pattern is repeated in the same order. The energy is calculated using (3).

$$Ene = \sum_{i=0}^{G-1} \sum_{j=0}^{G-1} Co(i, j)^2 \tag{3}$$

Entropy: The entropy feature gives content information for a texture image. Entropy value of non-specific and wide empty is low. Entropy value is higher in scattered areas with varying pixel values. Entropy is calculated using (4).

$$Ent = \sum_{i=0}^{G-1} \sum_{j=0}^{G-1} - Co(i, j) * \log Co(i, j) \tag{4}$$

Homogeneity: Homogeneity is also known as the inverse difference moment. When the homogeneity formula in (5) is examined, it is observed that, contrary to the contrast weights, homogeneity weights decrease exponentially when moving away from the GLCM diagonal.

$$Hom = \sum_{i=0}^{G-1} \sum_{j=0}^{G-1} \frac{1}{1 + (i - j)^2} Co(i, j) \tag{5}$$

Moment: Moment value is a measure indicating the uniform repeatability of texture. Moment is calculated using (6).

$$Mom = \sum_{i=0}^{G-1} \sum_{j=0}^{G-1} \frac{Co(i, j)^2}{1 + |i - j|} \tag{6}$$

Gabor filters are also used in the analysis of textural patterns. The human vision system (HVS) is sensitive to both specific orientation and spatial frequencies. For the analysis of textural patterns on the images, the frequency and direction sensitivity model for HVS can be performed with the wavelets. Textural feature extraction can be performed using a Gabor filter bank consisting of filters created at different frequencies and for different directions [21].

In the Gabor filter design, the highest frequency (f_m), the total number of frequencies (n_f) and the total number of routings (n_o) are defined first. Then filter bank is formed by creating different filters with combinations of frequency and routing parameters. Gabor filter-based feature extractors transfer images from their actual space to a feature space where they are represented by their own features. In (2) showing the Gabor filter formation, λ symbolizes the wavelength of the sinusoidal multiplier, θ symbolizes the angle value between 0 and 360 degrees indicating the normal orientation of the parallel lines of the Gabor function, φ symbolizes the cosine multiplier of the Gabor function, σ symbolizes the standard deviation of the Gaussian multiplier, γ symbolizes the aspect ratio that determines the ellipsoidality of the Gabor function in (7) [21]-[23].

$$G_{\lambda\theta\varphi\sigma\gamma}(x, y) = e^{-\frac{\dot{x}^2 + \dot{y}^2}{2\sigma^2}} \cos(2\pi \frac{\dot{x}}{\lambda} + \varphi)$$

$$\dot{x} = x \cos \theta + y \sin \theta \tag{7}$$

$$\dot{y} = -x \sin \theta + y \cos \theta$$

Gabor energy, which is closely related with the local power spectrum, is obtained by combining the outputs of a symmetric and antisymmetric kernel filter at a single value for each point of the image. This feature can be defined with (8).

$$e_{\lambda,\theta}(x, y) = \sqrt{r_{\lambda,\theta,0}^2(x, y) + r_{\lambda,\theta,-(1/2)\pi}^2(x, y)} \tag{8}$$

The features giving information about the presence or absence of dominant textural orientations are the real and imaginary parts of the complex moments of the local power spectrum. This feature can be calculated with (9).

$$C_{mn}(x, y) = \iint (u + iv)^m (u - iv)^n \tilde{p}_{u,v}(x, y) dudv, \tag{9}$$

$$m, n \in N$$

$$u = \frac{1}{\lambda} \cos \theta, v = \frac{1}{\lambda} \sin \theta, \tilde{p}_{u,v}(x, y) = p_{\lambda,\theta}(x, y)$$

The features obtained at each part of the image are saved and used in the training and testing of classification algorithms.

C. Figures

In the classification stage, the features extracted were used with three different classifiers trained. These are support vector machines, K-nearest neighbor algorithm and random forest algorithm.

Support vector machines (SVM) is a classification vector based on the statistical learning theory offered by Boser, Vapnik and Guyon in 1992 for the first time. SVM creates a hyper plane to separate a data set into two categories. The qualities belonging to the data used to identify the hyper plane, are called as 'features'. The group of features defining this state is called as 'vector' [24].

The K nearest neighbor algorithm is a trained algorithm. It determines the closest 'k' number of neighbors of the data it will classify within such data. It determines that, the data belongs to the class with the greatest number of neighbors in this 'k' number of neighbors [25], [26].

The random forest is formed by bringing several decision trees together. Each tree is grown as much as possible without

pruning. To classify an object, the input vector is labeled by each tree in the forest. The forest assigns the class according to the best rated label [25],[26].

III. EXPERIMENTAL STUDIES

Experiments were carried out to measure the performance of the developed system. In these experiments, a CT colonography data set prepared by TCIA, which consisted of the images of 825 patients, was used. In this data set, the data obtained from images of 50 randomly selected patients were used in the training of classification algorithms. The images of another 50 randomly selected patients were used for testing purposes.

Analysis of the results showed that, the performance rates of the system increased when the textural features obtained from the outer surfaces of the polyps were included in the classification process.

Comparison of classification algorithms revealed out that support vector machines reached better results. But there is no obvious superiority. The confusion matrix without outer surface textural features is presented in table V. In table VI, performance rates of the system without outer surface textural features are presented. The confusion matrix and performance rates of the system including outer surface textural features are presented in table VII and table VIII respectively.

TABLE V: CONFUSION MATRIX WITHOUT USING OUTER SURFACE TEXTURAL FEATURES

Algorithm	Polyps			Not Polyps		
	True	False	Total	True	False	Total
SVM	143	13	156	275	39	314
RF	133	23	156	264	50	314
KNN	135	21	156	270	44	314

TABLE VI: PERFORMANCE RATES WITHOUT USING OUTER SURFACE TEXTURAL FEATURES

Algorithm	Sensitivity	Selectivity	Accuracy
SVM	91,6%	87,5%	88,9%
RF	85,2%	84,1%	84,5%
KNN	86,5%	85,9%	86,2%

TABLE VII: CONFUSION MATRIX WITH USING OUTER SURFACE TEXTURAL FEATURES

Algorithm	Polyps			Not Polyps		
	True	False	Total	True	False	Total
SVM	151	5	156	287	27	314
RF	143	13	156	272	44	314
KNN	146	10	156	277	37	314

TABLE VIII: PERFORMANCE RATES WITH USING OUTER SURFACE TEXTURAL FEATURES

Algorithm	Sensitivity	Selectivity	Accuracy
SVM	96,7%	91,4%	93,0%
RF	91,6%	86,6%	88,2%
KNN	93,6%	88,2%	90,0%

IV. CONCLUSION

In this study, a CAD system that makes classification by extracting 3 different groups of features from CT images is

developed. The system aims to help radiologists determine whether the region of interest examined is a polyp candidate or not. The results revealed out that, outer surface textural features extracted by the system improved performance in determining suspicious polyps. The accuracy rates showed that the system might be ideal for clinical use.

In future studies, researchers could prefer a method that will use the more effective ones among the features and eliminate those which are less effective on the results. Furthermore, better results can be obtained in feature extraction stage by improving the pre-processing stage.

REFERENCES

- [1] R. L. Siegel, K.D. Miller, and A. Jemal, "Cancer statistics," *CA: A Cancer Journal for Clinicians*, 68: 7-30, 2018.
<https://doi.org/10.3322/caac.21442>
- [2] Cancer Facts & Figures 2018
- [3] D.M. Eddy, "Screening for colorectal cancer," *Annals of Internal Medicine*, vol. 113 No.5, pp. 373-384, 1990.
<https://doi.org/10.7326/0003-4819-113-5-373>
- [4] A. Mittal and K. Manjjeet, "Computer-aided-diagnosis in colorectal cancer: A survey of state of the art techniques," *International Conference on Inventive Computation Technologies (ICICT)*, Vol. 1. IEEE, 2016.
- [5] K. N. Manjunath, K. Gopalakrishna Prabhu, and P. C. Siddalingaswamy. "A knowledge based approach for colon segmentation in CT colonography images." *IEEE International Conference on Signal and Image Processing Applications (ICSIPA)*, IEEE, 2015.
- [6] J. Li, A. Huang, J. Yao, J. Liu, R.L.V. Uitert, N. Petrick, R.M. Summers, "Optimizing computer-aided colonic polyp detection for CT colonography", *Medical physics* vol. 36, No. 1, pp. 201-212, 2009.
<https://doi.org/10.1118/1.3040177>
- [7] T.A. Chowdhury and P. F. Whelan. "A fast and accurate method for automatic segmentation of colons at CT colonography based on colon geometrical features," *Irish Machine Vision and Image Processing Conference (IMVIP)*, IEEE, 2011.
- [8] C.L. Wyatt, Y. Ge, and D. J. Vining. "Automatic segmentation of the colon for virtual colonoscopy." *Computerized medical imaging and graphics*, vol.24, No.1, pp 1-9, 2000.
[https://doi.org/10.1016/S0895-6111\(99\)00039-7](https://doi.org/10.1016/S0895-6111(99)00039-7)
- [9] K. N. Manjunath, K. Gopalakrishna Prabhu, and P. C. Siddalingaswamy. "An expert system for electronic cleansing of contrast in CT colonography images." *IEEE International Conference on Signal and Image Processing Applications (ICSIPA)*, IEEE, 2015.
- [10] Y. Hu, B. Song, M. Ma, Z. Liang, "An application of KL transform in feature extraction and selection for polyp differentiation via CT colonography," *Nuclear Science Symposium and Medical Imaging Conference (NSS/MIC)*, IEEE, 2014.
- [11] Y. Ren, J. Ma, J. Xiong, Y. Chen, L. Lu, J. Zhao, "Improved False Positive Reduction by Novel Morphological Features for Computer-Aided Polyp Detection in CT Colonography." *IEEE Journal of Biomedical and Health Informatics*, Vol.22, No. 1, 2018.
<https://doi.org/10.1109/JBHI.2018.2808199>
- [12] J. Xu and K. Suzuki, "Max-AUC feature selection in computer-aided detection of polyps in CT colonography." *IEEE J. Biomedical and Health Informatics*, vol. 18.2 pp. 585-593, 2014.
- [13] S.H Bae and Y. Kuk-Jin, "Polyp detection via imbalanced learning and discriminative feature learning," *IEEE transactions on medical imaging*, vol. 34.11 pp. 2379-2393, 2015.
- [14] Ö. Demir and A.Y. Çamurcu. "Computer-aided detection of lung nodules using outer surface features." *Bio-medical materials and engineering* vol. 26. No. 1, pp. 1213-1222, 2015.
- [15] P.A. Devijver, "Connected components in binary images: the detection problem," John Wiley & Sons, Inc., 1984.
- [16] L. Di Stefano, A. Bulgarelli, A. "A Simple and Efficient Connected Components Labeling Algorithm," *International Conference on Image Analysis and Processing Proceedings*, 322-327, 1999.
<https://doi.org/10.1109/ICIAP.1999.797615>
- [17] D. S. Paik, C. F. Beaulieu, G. D. Rubin, B. Acar, R. B. Jeffrey Jr, J. Yee, J. Dey, S. Napel, "Surface Normal Overlap: A Computer-Aided Detection Algorithm with Application to Colonic Polyps and Lung Nodules in Helical Ct," *IEEE Transactions on Medical Imaging*, vol. 23, pp. 661-675.
<https://doi.org/10.1109/TMI.2004.826362>
- [18] R. N. Strickland, "Image-processing techniques for tumor detection," CRC Press, 2002.
<https://doi.org/10.1201/9780203909355>
- [19] M. Tuceryan and A. K. Jain, "Texture analysis in Handbook of pattern recognition and computer vision," pp. 235-276, 1993.
https://doi.org/10.1142/9789814343138_0010
- [20] R. M. Haralick and K. Shanmugam, "Textural features for image classification," *Transactions on systems, man, and cybernetics*, vol. 6, pp. 610-621, 1973.
- [21] F. Bianconi and A. Fernández. "Evaluation of the effects of Gabor filter parameters on texture classification," *Pattern Recognition* vol. 40.12 pp. 3325-3335, 2007.
- [22] Y. Wicaksono, R. S. Wahono and V. Suhartono, "Color and texture feature extraction using gabor filter-local binary patterns for image segmentation with fuzzy C-means," *Journal of Intelligent Systems*, vol. 1, no. 1, pp. 15-21, 2015
- [23] Ö. Demir and B. Doğan. "Unsupervised Image Segmentation Using Textural Features." *International Journal of Signal Processing Systems*, vol. 5, No. 3, pp. 112-115, 2017
<https://doi.org/10.18178/ijsp.5.3.112-115>
- [24] B.E. Boser, I. M. Guyon, V. N. Vapnik, "A Training Algorithm for Optimal Margin Classifiers," *Proceedings of the fifth annual workshop on Computational learning theory*, pp. 144-152, 1992.
- [25] C. C. Aggarwal, "Data classification: algorithms and applications," CRC Press, 2014.
<https://doi.org/10.1201/b17320>
- [26] N. M. Nasrabadi, "Pattern recognition and machine learning." *Journal of electronic imaging*, vol. 16 No. 4, 2007.
- [27] The Cancer Imaging Archive (2018) www.cancerimagingarchive.net (2018)



Önder Demir was born in İstanbul in 1980. received the MS and PhD degrees in Electronics and Computer Education from Marmara University in 2006 and 2013, respectively.

He worked as research assistant and lecturer from 2002 to 2013 Marmara University, Technical Education Faculty. He served in the military in 2013 and 2014. He served as an instructor at the Marmara University Technology Faculty between 2015 and 2017. He has been working as an Assistant Professor in Computer Engineering Department of Marmara University Technology Faculty since 2017. His research interests are digital image processing, biomedical image processing and algorithms.